Analyses

We determined the population size of the bacteriophage by adding 30 μl of chloroform to a 1 ml subsample of each chemostat (to remove bacteria) and plating 100 μl of the purified subsample of bacteriophage with 300 μl of an overnight culture of bacteria in 3 ml of soft agar. We counted the number of plaques (spots cleared of bacteria by the bacteriophage) after 24 h. Because the bacteriophage were well mixed before plating, each plaque was presumed to result from a single viral particle. A lawn of ancestral bacteria (B_0) was used to determine the total size of the bacteriophage population and a lawn of resistant bacteria (B_1) was used to calculate the number of host-range mutants ($T7_1$) in the bacteriophage population.

We determined the population size of the bacteria by plating 100 μl of a subsample (without chloroform treatment) and counting the number of bacterial colonies present after 24 h of incubation. To determine the size of the B_1 population, we plated the bacteria with an equal volume of ancestral bacteriophage.

To investigate local adaptation in the bacteriophage through time, we isolated two to three colonies of B_1 from the same day (day 9, 13 and 19) from each treatment during each run of the experiment. For each adaptation assay, overnight cultures of the colonies were grown up in 1 mg ml^{-1} glucose media. We plated replicate samples of $T7_1$ from each time point on a lawn of sympatric (from the same chemostat) and allopatric (from a different chemostat, but at the same productivity level) B_1 from the overnight culture. We used the 'efficiency of plating' (the number of plaques on each host) as a measure of bacteriophage infectivity.

We calculated adaptation as the ratio of the number of plaques formed by the numerically dominant bacteriophage on the dominant sympatric host to the number of plaques formed on the allopatric host. Ratios of the number of plaques formed on the bacterial isolates from each replicate run of the experiment were averaged to give a mean ratio for each run. Only one replicate run of the experiment was used in assays of the closed/high productivity community due to contamination. There were often no plaques on allopatric hosts, therefore we coded the data by adding one to both the numerator and the denominator to allow calculation of a ratio. A value above one indicates local adaptation and a number below one indicates local maladaptation (that is, the number of plaques was higher on the allopatric host than on the sympatric host). All ratios were log-transformed before analysis.

Variation in adaptation was assessed by calculating the coefficient of variation of the adaptation ratios. Significance was tested using an *F*-test, with a sequential Bonferroni correction for five pairwise comparisons[25]. Inspecting the data in detail showed that the reversed pattern for the open and closed intermediate productivity communities was driven by one of the two replicate runs of the experiment. Thus, we did not include data from the intermediate productivity communities in the analyses.

Received 3 July; accepted 30 July 2004; doi:10.1038/nature02906.

1. Thompson, J. N. *The Coevolutionary Process* (Univ. of Chicago Press, Chicago, 1994).
2. Brodie, E. D. Jr, Ridenhour, B. J. & Brodie, E. D. III The evolutionary response of predators to dangerous prey: hotspots and coldspots in the geographic mosaic of coevolution between garter snakes and newts. *Evolution* **56,** 2067–2082 (2002).
3. Burdon, J. J. & Thrall, P. H. Spatial and temporal patterns in coevolving plant and pathogen associations. *Am. Nat.* **153,** S15–S33 (2002).
4. Zangerl, A. R. & Berenbaum, M. R. Phenotype matching in wild parsnip and parsnip webworms: causes and consequences. *Evolution* **57,** 806–815 (2003).
5. Thompson, J. N. & Cunningham, B. M. Geographic structure and dynamics of coevolutionary selection. *Nature* **417,** 735–738 (2002).
6. Benkman, C. W., Parchman, T. L., Favis, A. & Siepielski, A. M. Reciprocal selection causes a coevolutionary arms race between crossbills and lodgepole pine. *Am. Nat.* **162,** 182–194 (2003).
7. Nuismer, S. L., Thompson, J. N. & Gomulkiewicz, R. Gene flow and geographically structured coevolution. *Proc. R. Soc. Lond. B* **266,** 605–609 (1999).
8. Hochberg, M. & van Baalen, M. Antagonistic coevolution over productivity gradients. *Am. Nat.* **152,** 620–634 (1998).
9. Chao, L., Levin, B. R. & Stewart, F. M. A complex community in a simple habitat: an experimental study with bacteria and phage. *Ecology* **58,** 369–378 (1977).
10. Lenski, R. E. & Levin, B. R. Constraints on the coevolution of bacteria and virulent phage: a model, some experiments, and predictions for natural communities. *Am. Nat.* **125,** 585–602 (1985).
11. Shrag, S. J. & Mittler, J. E. Host–parasite coexistence: the role of spatial refuges in stabilizing bacteria-phage interactions. *Am. Nat.* **148,** 348–377 (1996).
12. Bohannan, B. J. M. & Lenski, R. E. The relative importance of competition and predation varies with productivity in a model system. *Am. Nat.* **156,** 329–340 (2000).
13. Buckling, A. & Rainey, P. B. Antagonistic coevolution between a bacterium and a bacteriophage. *Proc. R. Soc. Lond. B* **269,** 931–936 (2002).
14. Thompson, J. N. The evolution of species interactions. *Science* **284,** 2116–2118 (1999).
15. Bohannan, B. J. M. & Lenski, R. E. The effect of resource enrichment on a chemostat community of bacteria and phage. *Ecology* **78,** 2303–2315 (1997).
16. Gandon, S. Local adaptation and the geometry of host–parasite coevolution. *Ecol. Lett.* **5,** 246–256 (2002).
17. Gandon, S. & Michalakis, Y. Local adaptation, evolutionary potential and host–parasite coevolution: interactions between migration, mutation, population size and generation time. *J. Evol. Biol.* **15,** 451–462 (2002).
18. Gomulkiewicz, R., Thompson, J. N., Holt, R. D., Nuismer, S. L. & Hochberg, M. E. Hot spots, cold spots and the geographic mosaic theory of coevolution. *Am. Nat.* **156,** 156–174 (2000).
19. Slatkin, M. Gene flow in natural populations. *Annu. Rev. Ecol. Syst.* **16,** 393–430 (1985).
20. Futuyma, D. J. *Evolutionary Biology,* 3rd edn (Sinauer Associates Inc., Sunderland, 1998).
21. Gandon, S., Capowiez, Y., Dubios, Y., Michalakis, Y. & Olivieri, I. Local adaptation and gene-for-gene coevolution in a metapopulation model. *Proc. R. Soc. Lond. B* **263,** 1003–1009 (1996).
22. Buckling, A., Wills, M. A. & Colegrave, N. Adaptation limits diversification of experimental bacterial populations. *Science* **302,** 2107–2109 (2003).
23. Brockhurst, M. A., Morgan, A. D., Rainey, P. B. & Buckling, A. Population mixing accelerates coevolution. *Ecol. Lett.* **6,** 975–979 (2003).
24. Bohannan, B. J. M. & Lenski, R. E. Effect of prey heterogeneity on the response of a model food chain to resource enrichment. *Am. Nat.* **153,** 73–82 (1999).
25. Rice, W. R. Analyzing tables of statistical tests. *Evolution* **43,** 223–225 (1989).

Acknowledgements We thank B. Kerr, E. Danner and members of the Thompson and Bohannan laboratories for comments on previous drafts of this manuscript. We are grateful to P. Raimondi for assistance with data analysis.

Competing interests statement The authors declare that they have no competing financial interests.

Correspondence and requests for materials should be addressed to S.E.F. (forde@biology.ucsc.edu).

Hedgehog signalling controls eye degeneration in blind cavefish

Yoshiyuki Yamamoto[1]*, David W. Stock[2] & William R. Jeffery[1]

[1]*Department of Biology, University of Maryland, College Park, Maryland 20742, USA*
[2]*Department of Ecology and Evolutionary Biology, University of Colorado, Boulder, Colorado 80309, USA*

* Present address: Evolutionary Anatomy Unit, Department of Anatomy & Developmental Biology, University College London, Gower Street, London WC1E 6BT, UK

Hedgehog (Hh) proteins are responsible for critical signalling events during development[1] but their evolutionary roles remain to be determined. Here we show that *hh* gene expression at the embryonic midline controls eye degeneration in blind cavefish. We use the teleost *Astyanax mexicanus*, a single species with an eyed surface-dwelling form (surface fish) and many blind cave forms (cavefish)[2], to study the evolution of eye degeneration. Small eye primordia are formed during cavefish embryogenesis, which later arrest in development, degenerate and sink into the orbits. Eye degeneration is caused by apoptosis of the embryonic lens, and transplanting a surface fish embryonic lens into a cavefish optic cup can restore a complete eye[3–5]. Here we show that *sonic hedgehog* (*shh*) and *tiggy-winkle hedgehog* (*twhh*) gene expression is expanded along the anterior embryonic midline in several different cavefish populations. The expansion of *hh* signalling results in hyperactivation of downstream genes, lens apoptosis and arrested eye growth and development. These features can be mimicked in surface fish by *twhh* and/or *shh* overexpression, supporting the role of *hh* signalling in the evolution of cavefish eye regression.

Cave animals often lose their eyesight during evolution in perpetual darkness (Fig. 1a, b), but the evolutionary and developmental mechanisms underlying these dramatic phenotypes are unknown[6]. Over the last 10,000 yr, at least four different *Astyanax* cavefish populations may have evolved various degrees of eye degeneration independently[7–10]. In addition to blindness, cavefish show other regressive and constructive morphological features, including loss of melanin pigment, modifications in the orbital skeleton and increases in jaw size, maxillary teeth and taste buds[2,10]. We previously reported that *pax6* expression is downregulated in the presumptive optic fields in several cavefish populations, suggesting that upstream regulators of *pax6* may control eye degeneration[11].

To detect early changes in eye development, optic morphogenesis and gene expression patterns were compared in cavefish and surface fish embryos. The results showed that the optic vesicle is reduced in size (Fig. 1c, d) and the ventral sector of the optic cup is lost (Fig. 1e, f)

in cavefish embryos. Vertebrate optic primordia are patterned by reciprocal transcriptional repression between the transcription factors Pax2, which is expressed in the optic stalk, and Pax6, which is expressed in the optic cup[12,13]. *In situ* hybridization showed that *pax2a* expression is expanded in the cavefish optic vesicle and optic cup (Fig. 1c, d, g, h). Changes in the optic primordium were confirmed by examining *vax1*, which is also expressed in the optic stalk[14,15]. Similar to *pax2a*, *vax1* expression was expanded in the cavefish optic cup (Fig. 1i, j), suggesting that upregulation of these genes modifies the eye primordia.

Hh proteins emanating from the anterior embryonic midline control the expression of *pax2*, *vax1* and *pax6* in vertebrate optic primordia[13–17]. Comparisons of *hh* gene expression in surface fish and cavefish embryos revealed several highly reproducible changes along the anterior midline. At the neural plate stage, *shh* and *twhh* expression was expanded in the cavefish prechordal plate relative to non-overlapping *pax2a* expression at the future midbrain–hindbrain boundary[18] and *dlx3b* expression at the border of the neural plate[19] (Fig. 2a–d, i–j). The cavefish *shh*-expressing domain is about ten cells wide at its greatest lateral extent, whereas it is only about six cells wide in surface fish ($n = 6$). During optic vesicle formation, *shh* expression extended further anterior and dorsal in cavefish, curling around the rostrum (Fig. 2e–h). To confirm *hh* expansion, we also examined the expression patterns of *hh* downstream target genes. The results showed that *ptc2* (Fig. 2k, l), which encodes a *shh* receptor[20,21], and *nkx2.1a* (Fig. 2m, n), which encodes an *hh*-regulated transcription factor[22], were also expanded along the cavefish midline. The significance of *hh* expansion in eye loss was established in two ways. First, two additional cavefish populations

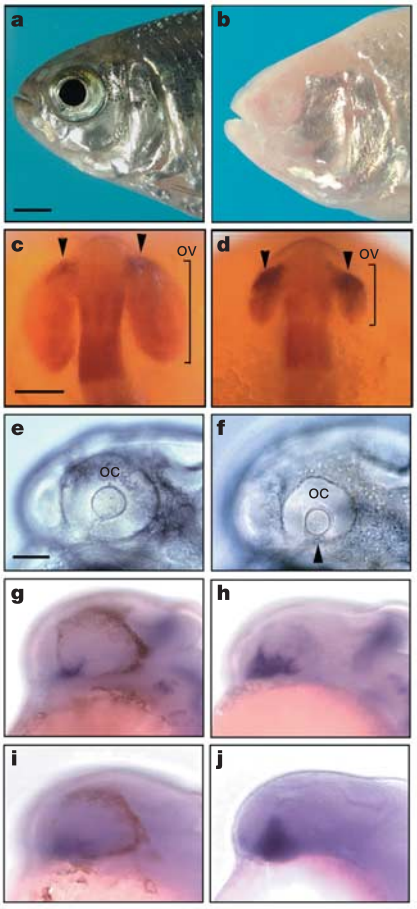

Figure 1 Changes in surface fish (left column) and cavefish (right column) eyes and optic primordia. **a**, **b**, Adults. **c**, **d**, *pax2a* expression (arrowheads) in optic vesicles (ov). **e**, **f**, Optic cup (oc) morphology showing loss of ventral sector (arrowhead) in cavefish. **g**–**j**, *pax2a* (**g**, **h**) and *vax1* (**i**, **j**) expression in optic vesicles. Shown are dorsal (**c**, **d**) and lateral (**a**, **b**, **e**–**j**) views with anterior on left. Scale bars: 0.5 cm (**a**), 250 μm (**c**) and 150 μm (**e**); same magnification in **a** and **b**, **c** and **d** and **e**–**j**.

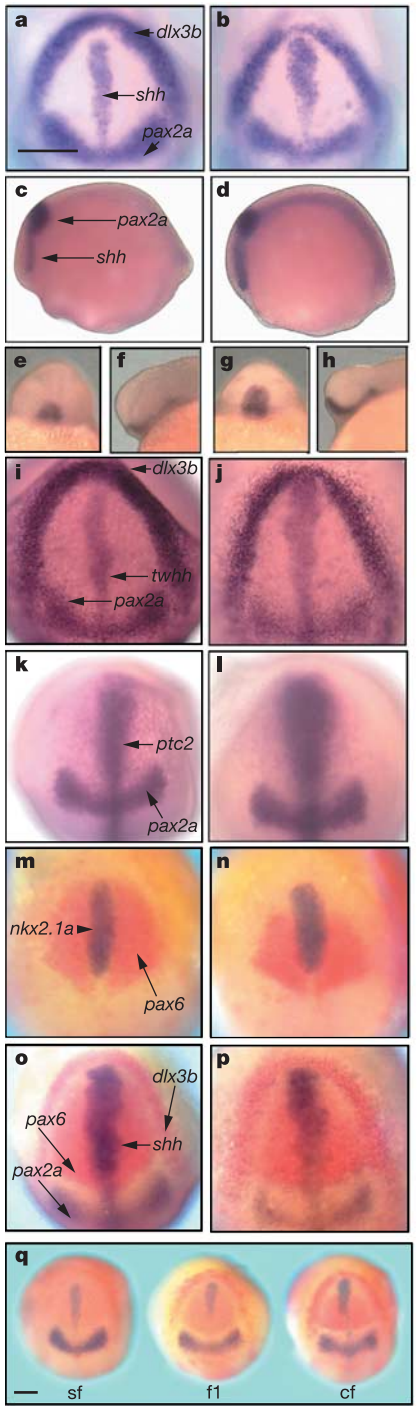

Figure 2 *hh* and *hh*-related gene expression in fish embryos. (Surface fish: **a**, **c**, **e**, **f**, **i**, **k**, **m**; cavefish: **b**, **d**, **g**, **h**, **j**, **l**, **n**–**p**.) **a**–**j**, *shh* (**a**–**h**) and *twhh* (**i**, **j**) expression relative to *dlx3b* and/or *pax2a* expression in early tailbud (**a**–**d**, **i**, **j**) and 10-somite (**e**–**h**) embryos. **k**–**n**, *ptc2* (**k**, **l**) and *nkx2.1a* (**m**, **n**) expression relative to *pax2a* and *pax6* expression respectively in early tailbud embryos. **o**–**q**, *shh* (blue) expression relative to *dlx3b* (red), *pax2a* (blue) and *pax6* (red) expression in early tailbud-stage Chica (**o**) and Los Sabinos (**p**) cavefish embryos and surface fish (sf), F1 (f1) and cavefish (cf) embryos (**q**). Shown are dorsal (**a**, **b**, **i**–**q**), lateral with anterior on left (**c**, **d**, **f**, **h**) and rostral (**e**, **g**) views. Scale bars, 250 μm; same magnification in **a**–**p**.

were examined and these also exhibited expansion of *shh* expression at the embryonic midline (Fig. 2o, p). Second, *shh* expression was examined in the progeny of a cross between surface fish and cavefish. The F1 embryos, which have uniformly small eyes relative to surface fish[2,23], showed a midline *shh* domain intermediate in width between surface fish and cavefish (Fig. 2q).

To test the possibility that eye degeneration is caused by increased Hh signalling, we overexpressed *hh* by injecting *twhh* and/or *shh* messenger RNA into surface fish embryos[16]. As a result, *shh* and *nkx2.1a* expression were expanded at the anterior midline and *pax6* expression was contracted in the presumptive optic regions of the injected embryos (Fig. 3a–c; data not shown). Subsequently, smaller optic vesicles (Fig. 3f) with expanded *pax2a* (data not shown) and *vax1* (Fig. 3d, e) expression and ventrally reduced optic cups (Fig. 3g) were observed. The affected features usually occurred unilaterally, probably because mRNA was injected on one side of the bilateral embryonic axis. However, the unilateral changes were observed in a proportion of embryos that paralleled those in which *shh* was expanded on only one side of the anterior midline. By the larval stage, 78% ($n = 50$) of these embryos exhibited a ventrally diminished retina and a small or undetectable lens (Fig. 3h). Adults that developed from these embryos were missing an eye (Fig. 3i) and did not respond to light focused on the affected orbit. *Shh* overexpression had no detectable effects on body pigmentation, the orbital skeleton, jaw width or maxillary tooth number, although there was a small increase in taste bud number on the lips (6%, $n = 30$). Similar effects were observed following injection of *shh*/*twhh* or *shh* mRNA. The results indicate that *hh* overexpression can phenocopy cavefish eye degeneration.

To determine the effects of reducing Hh activity, cavefish embryos were treated with cyclopamine, an inhibitor of the Hh signalling pathway[24]. Cyclopamine-treated embryos showed larger optic vesicles with diminished *pax2a* (data not shown) and *vax1* domains (Fig. 3j, k). Later in development, the lens was 30% larger than in controls ($n = 38$), supporting a partial restoration of eye development. However, eye development was not completely restored in cyclopamine-treated cavefish embryos, probably due to the late requirement for *shh* and *twhh* expression in the developing retina[25,26].

Further experiments were conducted to determine the effects of increased midline signalling on lens and eye development. First, 43% ($n = 42$) of the *shh* mRNA-injected embryos assayed by TdT-mediated dUTP nick end labelling assay (TUNEL)[3] exhibited apoptosis in one or both lens vesicles (Fig. 4a, b). Second, eye development was arrested in 36% ($n = 25$) of the cases in which a

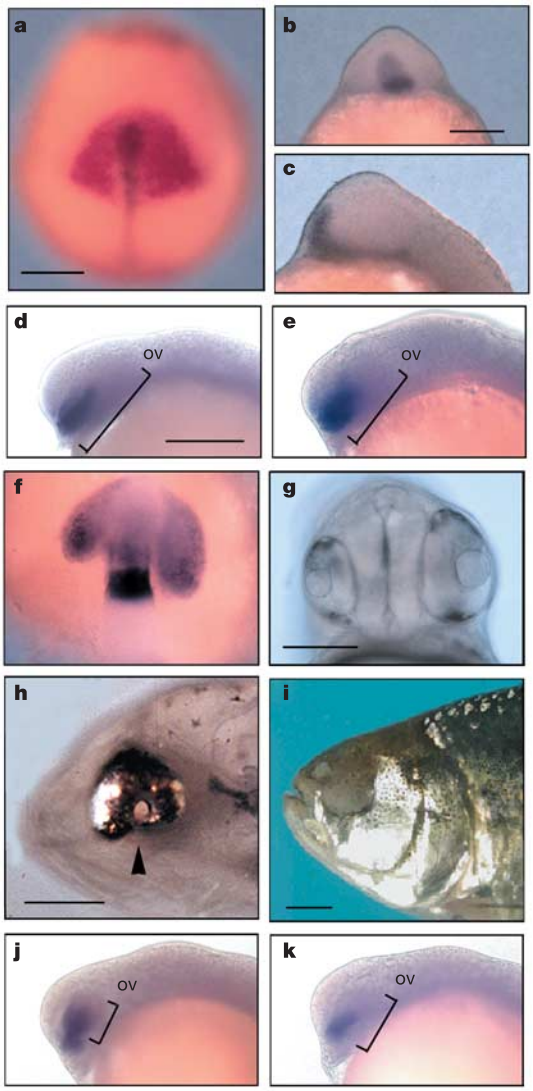

Figure 3 *hh* control of eye formation. **a**–**i**, Effects of *twhh* and *shh* (**a**–**c**, **f**–**i**) or *shh* (**e**) mRNA injection in surface fish embryos. **a**–**c**, Early tailbud (**a**) and 10-somite (**b**, **c**) embryos with expanded *shh* (blue) and asymmetric *pax6* expression (**a**, red). **d**, **e**, Expanded *vax1* expression in the optic vesicle (ov) of an *hh* mRNA-injected embryo (**e**) compared to a control (**d**). **f**, **g**, Unilateral reduction of optic vesicle (**f**, *pax6* staining) at the 18-somite stage and optic cup (**g**) at the hatching stage in *hh* mRNA-injected embryos. **h**, **i**, Ventral eye reduction (**h**, arrowhead) and eye loss in a blind cavefish phenocopy (**i**) after *hh* mRNA injection. **j**, **k**, *vax1* expression in cyclopamine-treated (**k**) and control (**j**) cavefish embryos. Shown are dorsal (**a**, **f**), lateral with anterior on left (**c**–**e**, **h**–**k**) and rostral (**b**, **g**) views. Scale bars: 200 μm (**a**), 250 μm (**b**, **d**), 150 μm (**g**), 100 μm (**h**) and 0.5 cm (**i**); same magnification in **b** and **c**, **d**–**f**, and **j** and **k**.

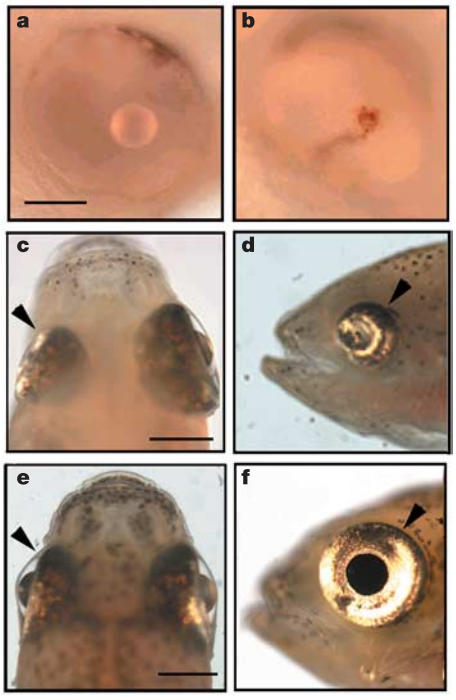

Figure 4 Effects of *shh* overexpression on surface fish lens development. **a**, **b**, TUNEL-positive apoptotic lens (red) in a *shh* mRNA-injected embryo (**b**) but not in a control (**a**). **c**, **d**, Inhibition of eye growth after lens transplantation from *shh* mRNA-injected embryo into the optic cup of a normal embryo. **e**, **f**, Restoration of eye growth after transplantation of a lens from a normal embryo into the affected optic cup of a *shh* mRNA-injected embryo. Arrowheads: transplantation side. Shown are dorsal (**c**, **e**) and lateral (**a**, **b**, **d**, **f**) views. Scale bars: 150 μm (**a**) and 100 μm (**c**, **e**); same magnification in **a** and **b**, **c** and **d**, and **e** and **f**.

lens was transplanted from a *shh* mRNA-injected surface fish embryo into the optic cup of a normal surface fish embryo (Fig. 4c, d). In contrast, eye development was not affected by lens transplantation from a normal surface fish embryo into the optic cup of another normal surface fish embryo (data not shown, $n = 118$). Third, eye development was partially or completely restored in 35% of the cases ($n = 17$) in which a normal lens was transplanted into the arrested eye of a *shh* mRNA-injected surface fish embryo (Fig. 4e, f). The results suggest that *shh* overexpression inhibits eye growth and development by inducing lens apoptosis.

We conclude that eye degeneration is mediated by expanded midline signalling in cavefish embryos. Accordingly, a small increase in Hh signalling at the embryonic midline is amplified by the induction of lens apoptosis to elicit a large negative effect on eye growth and development. Thus, *shh* and *twhh* could represent two of the four to six genes estimated to be involved in cavefish eye loss[23], although it is possible that upstream regulatory genes rather than *hh* genes themselves may be mutated during cavefish evolution. The latter hypothesis would explain coordinated changes in expression of the two *hh* paralogues.

Eye regression in cave animals has been attributed to loss-of-function mutations in eye genes, which may accumulate without penalty under conditions of relaxed selection for eyesight[6,23]. The control of eye degeneration by a gain of function in *hh* or related midline-signalling genes in *Astyanax* cavefish raises the alternative possibility that eye regression could be driven by natural selection for an adaptive trait(s). Understanding the adaptive significance of enhanced Hh signalling is expected to provide key insights into the mechanisms controlling the evolution of blind cavefish. □

Methods

Biological materials and procedures

A. mexicanus embryos were obtained as described previously[3–5,10,11]. All experiments were conducted with Pachón cavefish unless otherwise indicated.

Probes and *in situ* hybridization

Antisense RNA probes were generated from complete surface fish *shh* and *pax6* complementary DNAs, a partial *twhh* cDNA and *pax2a*, *dlx3b*, *vax1*, *ptc2* and *nkx2.1a* DNAs amplified from surface fish RNA by polymerase chain reaction (PCR) with reverse transcription. The *twhh* probe, which contains the 5′ UTR and part of the amino-terminal coding sequence of the mRNA, showed a different expression pattern than *shh* in developing fin buds and is therefore considered to be gene specific. The following oligo primers were used in PCR reactions: *pax2a* CAGCCTTTCCATCTATCTCCAG (forward) and CCGTAAACTCTCCACACTACCC (reverse), *dlx3b* GCCGGGATCCAARGAYTCN CCNACNYTNCC (forward) and GCCGGAATTCGARTTRCANGCCATNGARTC (reverse), *vax1* GCTCCATMCGRGARARATCAT (forward) and TTYTTCCTGCCTTT CCT (reverse), *ptc2* GTGTCTMTKTATGGAAAATCTTGG (forward) and TGACCTTACTCCTSTTTCGG (reverse) and *nkx2.1a* CTSCCRBCYTACCARGASRS (forward) and GCSGASAGGTAYTTYTGYTG (reverse). Two-colour *in situ* hybridizations[11] were done using digoxygenin-(blue) and fluorescein-(red) labelled RNA probes with the colour developed using NBT/BCIP or Fast Red respectively.

hh up- and downregulation

Constructs to produce mRNAs were made by inserting the full-length surface fish *shh* cDNA into the pSP64T plasmid. In some experiments we injected zebrafish *shh* and *twhh* mRNAs (1:1) made from pT7TS plasmids. The blastomeres of embryos at the 1–4-cell stage were injected with 0.4 ng nl^{-1} (2 nl total volume) *hh* mRNA or control green fluorescent protein mRNA. Embryos were treated with 20–100 μM cyclopamine (5 mM stock solution in 95% ethanol; Toronto Research Chemicals) from 30% epiboly to hatching.

Received 20 May; accepted 19 July 2004; doi:10.1038/nature02864.

1. Ingham, P. W. & McMahon, A. P. Hedgehog signaling in animal development: paradigms and principles. *Genes Dev.* **15,** 3059–3087 (2001).
2. Jeffery, W. R. Cavefish as a model system in evolutionary developmental biology. *Dev. Biol.* **231,** 1–12 (2001).
3. Jeffery, W. R. & Martasian, D. P. Evolution of eye regression in the cavefish *Astyanax*: Apoptosis and the *Pax6* gene. *Am. Zool.* **38,** 685–696 (1998).
4. Yamamoto, Y. & Jeffery, W. R. Central role for the lens in cavefish eye degeneration. *Science* **289,** 631–633 (2000).
5. Jeffery, W. R., Strickler, A. G. & Yamamoto, Y. To see or not to see: Evolution of eye degeneration in the Mexican blind cavefish. *Integr. Comp. Biol.* **43,** 531–541 (2003).
6. Culver, D. C. *Cave Life. Evolution and Ecology* (Harvard Univ. Press, Cambridge, 1982).
7. Mitchell, R. W., Russell, W. H. & Elliot, W. R. Mexican eyeless characin fishes, genus *Astyanax*: Environment, distribution, and evolution. *Spec. Publ. Mus. Texas Tech. Univ.* **12,** 1–89 (1977).
8. Dowling, T. E., Martasian, D. P. & Jeffery, W. R. Evidence for multiple genetic forms with similar eyeless phenotypes in the blind cavefish, *Astyanax mexicanus*. *Mol. Biol. Evol.* **19,** 446–455 (2002).
9. Strecker, U., Bernatchez, L. & Wilkens, H. Genetic divergence between cave and surface populations of *Astyanax* in Mexico (Characidae, Teleostei). *Mol. Ecol.* **12,** 699–710 (2003).
10. Yamamoto, Y., Stock, D. W. & Jeffery, W. R. Development and evolution of craniofacial patterning is mediated by eye-dependent and -independent processes in the cavefish *Astyanax*. *Evol. Dev.* **5,** 435–446 (2003).
11. Strickler, A. G., Yamamoto, Y. & Jeffery, W. R. Early and late changes in *Pax6* expression accompany eye degeneration during cavefish development. *Dev. Genes Evol.* **211,** 138–144 (2001).
12. Schwarz, M. *et al.* Spatial specification of mammalian eye territories by reciprocal transcriptional repression of Pax2 and Pax6. *Development* **127,** 4325–4334 (2000).
13. Macdonald, R. *et al.* Midline signalling is required for *Pax6* gene regulation and patterning of the eyes. *Development* **121,** 3267–3278 (1995).
14. Hallonet, M., Hollemann, T., Pieler, T. & Gruss, P. *Vax1*, a novel homeobox-containing gene, directs visual system development of the basal forebrain and visual system. *Genes Dev.* **13,** 3106–3114 (1999).
15. Take-uchi, M., Clarke, J. D. W. & Wilson, S. W. Hedgehog signalling maintains the optic stalk-retinal interface through the regulation of Vax gene activity. *Development* **130,** 955–968 (2003).
16. Ekker, S. C. *et al.* Patterning activities of vertebrate hedgehog proteins in the developing eye and brain. *Curr. Biol.* **5,** 944–955 (1995).
17. Li, H., Tierney, C., Wen, L., Wu, J. Y. & Rao, Y. A single morphogenetic field gives rise to two retinal primordia under the influence of the prechordal plate. *Development* **124,** 603–615 (1997).
18. Kelly, G. M. & Moon, R. T. Involvement of wnt1 and pax2 in the formation of the midbrain–hindbrain boundary in the zebrafish gastrula. *Dev. Genet.* **17,** 129–140 (1995).
19. Akimenko, M. A., Ekker, M., Wegner, J., Lin, W. & Westerfield, M. Combinatorial expression of three zebrafish genes related to distalless: part of a homeobox gene code for the head. *J. Neurosci.* **14,** 3475–3486 (1994).
20. Goodrich, L. V., Johnson, R. I., Milenkovic, L., McMahon, J. & Scott, M. Conservation of the hedgehog/patched signaling pathway from flies to mice: Induction of a mouse patched gene by hedgehog. *Genes Dev.* **10,** 301–312 (1996).
21. Marigo, V., Davey, R. A., Zuo, Y., Cunningham, J. M. & Tabin, C. J. Biochemical evidence that patched is the hedgehog receptor. *Nature* **384,** 176–179 (1996).
22. Pabst, O., Herband, H., Takuma, N. & Arnold, H. H. NKX2 gene expression in neuroectoderm but not mesodermally derived structures depends on sonic hedgehog in mouse. *Dev. Genes Evol.* **210,** 47–50 (2000).
23. Wilkens, H. Evolution and genetics of epigean and cave *Astyanax* (Characidae, Pisces). *Evol. Biol.* **23,** 271–367 (1988).
24. Incardona, J. P., Garfield, W., Kapur, R. P. & Roelink, H. The teratogenic *Veratrum* alkaloid cyclopamine inhibits Sonic hedgehog signal transduction. *Development* **125,** 3553–3562 (1998).
25. Neumann, C. J. & Nuesslein-Volhard, C. Patterning of the zebrafish retina by a wave of sonic hedgehog activity. *Science* **289,** 2137–2139 (2000).
26. Stenkamp, D. L., Frey, R. A., Prabhudesai, S. N. & Raymond, P. A. Function for Hedgehog genes in zebrafish retinal development. *Dev. Biol.* **220,** 238–252 (2000).

Acknowledgements We thank L. Law, A. Parkhurst, L. Reed and A. G. Strickler for assistance with sequencing and database submission, and R. T. Moon for providing pT7TS plasmids. This work was supported by grants from the National Science Foundation (D.W.S. and W.R.J.) and the National Institutes of Heath (W.R.J.).

Competing interests statement The authors declare that they have no competing financial interests.

Correspondence and requests for materials should be addressed to W.R.J. (jeffery@umd.edu). The *Astyanax* surface fish *pax6*, *shh*, *dlx3b*, *twhh*, *ptc2*, *nkx2.1a*, *pax2a* and *vax1* DNA sequences have been deposited in the GenBank database under accession numbers AY651762, AY661431, AY661432, AY661433, AY661434, AY661435, AY661436 and AY661437, respectively.

A relative signalling model for the formation of a topographic neural map

Michaël Reber, Patrick Burrola & Greg Lemke

Molecular Neurobiology Laboratory, The Salk Institute, La Jolla, California 92037, USA

The highly ordered wiring of retinal ganglion cell (RGC) neurons in the eye to their synaptic targets in the superior colliculus of the midbrain has long served as the dominant experimental system for the analysis of topographic neural maps[1–3]. Here we describe a quantitative model for the development of one arm of this map—the wiring of the nasal–temporal axis of the retina to the caudal–rostral axis of the superior colliculus. The model is based on